6TH INTERNATIONAL CONFERENCE ON FLOOD MANAGEMENT
September 2014 - São Paulo - Brazil
ICFM6

DEVELOPMENT OF A SNOWMELT-RUNOFF MODEL CONSIDERING DAM FUNCTION FOR THE ANE RIVER DAM BASIN, JAPAN

P.L.B. Chaffe[1], APIP[2], Y. Yamashiki[3] and K. Takara[3]

1. *Department of Sanitary and Environmental Engineering, Federal University of Santa Catarina, Brazil, pedro.chaffe@ufsc.br*
2. *Research Center for Limnology, Indonesian Institute of Sciences (LIPI), Indonesia*
3. *Disaster Prevention Research Institute, Kyoto University, Japan*

ABSTRACT: The Ane River Basin is located in Japan and snowmelt during spring is a major contribution to total river discharge. The proper estimation of the snowmelt runoff in the maritime snow area is necessary for the understanding of the hydrological processes of the region and for analyzing different climate change impacts in the water resources of the area. The objective of this paper was to develop and test an energy balance snowmelt and runoff model for the Ane River Dam catchment considering dam reservoir. The Ane River Dam (ARD) has a catchment area of 28 km^2 mainly covered by forest. The model developed was a combination of three different models: an energy-balance Soil-Vegetation-Atmosphere-Transfer model for the snowmelt calculation; a cell distributed runoff model (CDRMV3); and the implementation of a dam reservoir routing routine using the Level Pool method. In the model we set the grid cell where the dam is located to have the reservoir rules. The runoff model was calibrated by using dam inflow hydrographs for three summer events. Snow accumulation and depletion pattern represented well the observed snow depth at the crest of the ARD. The total snow depth was overestimated due to the constant snow density which was used in the model. The time of snow disappearance was well estimated for the winter of 2010-2011, however, it was 10 days late in the winter of 2010. The simulated peak outflow from the dam was overestimated but the recession curves were accurate. The use of the summer calibrated parameters for the three winter events demonstrates the developed snowmelt-runoff model sensitivity to snowmelt and rainfall. However, there are still verification limitations due to the quality of observed inflow data during the winter and the uncertain simulation of soil moisture patterns.

Key Words: Ane River Dam, Distributed Hydrological Model, Snowmelt, SVAT

1. INTRODUCTION

The hydrological cycle is controlled by physiographic, climatic and human factors. A change in one of those controls can severely affect the entire cycle and diminish our ability to predict its future states. It is expected that with climate change the hydrological cycle could change significantly due to changes in evaporation, precipitation patterns and others. Water resources management could be a challenging activity especially in places like Japan where river basins are highly populated and highly regulated. Japanese rivers are highly regulated and most of the dam operation depends on the reliable predictability of hydrological factors.

Lake Biwa is the largest freshwater body in Japan and it supplies water for more than 14 million people in the Kinki region. The North part of Lake is in a maritime climate and is considered very susceptive to climate change due to its significant snowfall and relatively warm temperatures in the winter. There are concerns about flood problems during the spring with rain-on-snow events and questions of whether if changes in the snow regime in the future could enhance such flood problems early in the spring or perhaps aggravate water scarcity during the summer are yet to be answered. The proper estimation of the snowmelt runoff in this area is necessary for the understanding of the hydrological processes of the

region and for analyzing different climate change scenarios impacts in the future of water resources. The objective of this paper was to develop and test an energy balance snowmelt and runoff model for the Ane River Dam catchment considering dam reservoir

2. THE ANE RIVER DAM BASIN

The Ane River Basin is located in the Northeast region of Shiga Prefecture (Figure 1) and it is the basin which contributes the largest discharge to Lake Biwa. It belongs to the Japan Sea climatic region and the average temperature of this region is 14.5 °C and the precipitation is around 2000 mm per year. The snowmelt during spring is a major contribution of total river discharge. The Ane River Dam (ARD) is a gravity dam built in the upstream part of the Ane River (Figure 1), its construction was finalized in March 2002. The crest of the dam sits at an elevation of 450 m and the catchment area is about 28 km2. The main purpose of the ARD is to provide irrigation water and for flood control. The land use is mainly composed of forest.

The Dam has three outlets, one minor controlled outlet which should maintain normal function of river discharge is operated when water level is between elevation 427.4 m and 413.0 m. The main flood control spillway is not controlled and is the main outlet for the water elevation between 427.4 m and 446.7 m. Water above the elevation of 446.7 m will be spilled by the emergency spillways which sit on top of the dam crest.

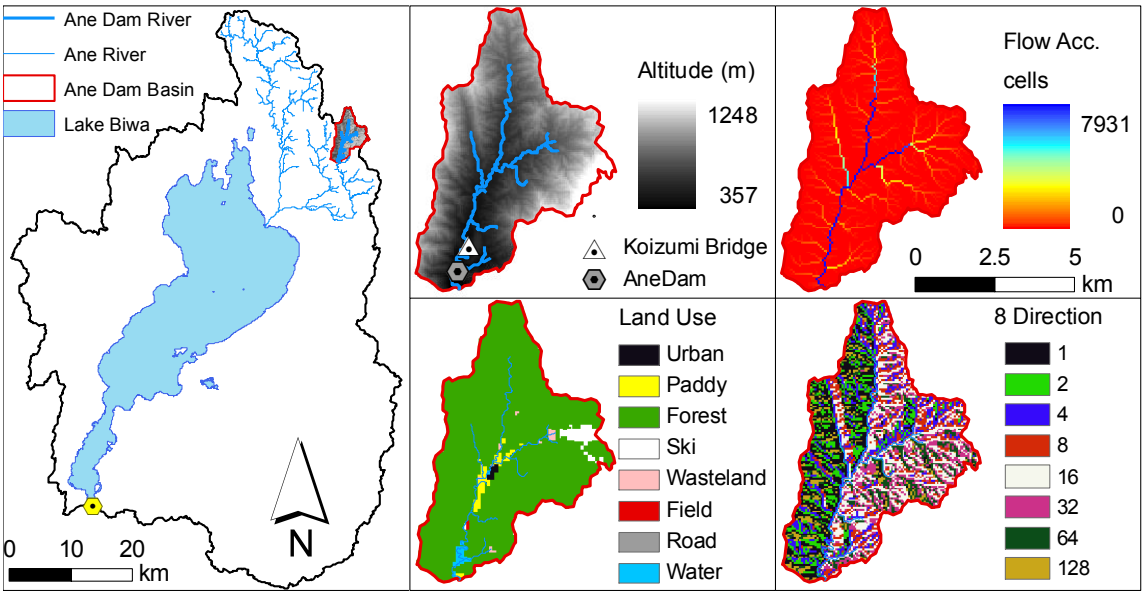

Figure 1: Location map of the Ane River Dam basin and maps used as input for the distributed runoff model (DEM, flow accumulation, land use and eight direction flow map).

3. HYDROMETEOROLOGICAL DATA

Hourly water level inside the Dam, water inflow and outflow of the dam for the periods of January 2010 to April 2011 were provided by the Ane Dam management office. Inflow discharge for winter periods are not reliable due to possible freezing of water in Koizumi bridge where staff gage station is installed.

We used radar-AMeDAS precipitation product provided by Japan Meteorological Agency (JMA). The radar-AMeDAS precipitation intensity map is based on radar echo intensity operated around Japan combined with about 1300 observed raingauges which are part of the Automated Meteorological Data

Acquisition System (AMeDAS). Radar-AMeDAS is calibrated with AMeDAS raingauges and the estimates from different radars (Makihara 1996). Observations are often obstructed by mountains, therefore the precipitation estimates are computed by removing the orographic effect and integrating the observations (Oki and Sumi 1994, Makihara 1996).

Radar-AMeDAS data has been used in many different hydrological application and for estimating precipitation observation errors from different satellites (Oki and Sumi 1994, Oki et al. 1997, Shimizu et al. 2001, Iida et al. 2006). The overall accuracy is reliable especially in intense precipitation, however precipitation estimates tend to be larger than observations (Kitabake and Obayashi 1991). Urita et al. (2011) showed the high accuracy for short term precipitation estimates of radar-AMeDAS and that the discontinuities for long term estimates are due to different interpolation methods and spatial resolution used in different periods. For the period of 2010-2011, thirty minute rainfall intensity were available and converted to hourly precipitation volumes. The spatial resolution is of approximately 1km. Despite the recent improvements in the precipitation estimates due to use of more radar and raingauges, there is no error estimates for the winter time.

Temperature and sunlight hours were obtained integrating 10min data from AMeDAS stations to hourly values. Temperature, radiation, atmospheric pressure, relative humidity, wind speed and snow depth at the ARD crest were provided by the Ane Dam management office.

4. SNOMELT-RUNOFF MODEL

In the development of the snowmelt-runoff model for this study we modified and combined three different models: an energy-balance Soil-Vegetation-Atmosphere-Transfer *SVAT* model (Ma *et al*. 2003, Sato *et al*. 2008) for the snowmelt calculation; a cell distributed runoff model (Kojima and Takara 2003) which uses snowmelt and rainfall input from the SVAT model; and the implementation of a dam reservoir routing routine using the Level Pool method.

4.1 Snowmelt Model

The separation of total precipitation into snow (P_s) and rain was made using an empirical relationship Eq. (1) (Iwaki et al. 2011). That is the first step for the snow accumulation model.

$$\begin{cases} P_s = P \cdot \dfrac{a}{100} & a = -17.63\ T + 86.61 \quad (-0.8 \le T \le 4.9) \\ P_s = P & (T < -0.8) \\ P_s = 0 & (T > 4.9) \end{cases} \qquad [1]$$

P is the total precipitation (mm h^{-1}), T is the ground air temperature (°C) and a is the probability of occurrence of solid precipitation (%). The relation between a and T (°C) was derived by using data obtained from meteorological observations carried out in the city of Hikone, which is located in the eastern part of Shiga Prefecture.

In the SVAT model (Ma et al. 2003, Sato et al. 2008) the snowmelt is calculated using the energy balance method. The energy balance method used in this study was developed, modified and applied in several conditions (Kondo and Yamazaki 1990, Yamazaki and Kondo 1992, Kondo and Xu 1997, Ma et al. 1998, 1999, 2000, 2003, Xu et al. 2005, Sato et al. 2008). This explanation mainly follows Ma et al. (2003) and Sato et al. (2008). The energy balance on the surface can be expressed as:

$$R_n = H + \lambda E + G \qquad [2]$$

where R_n (W m^{-2}) is the net radiation, H (W m^{-2})is the sensible heat flux, λE (W m^{-2}) is the latent heat flux and G is the soil and snow heat flux.

4.2 Cell Distributed Runoff Model

A one dimensional physically based distributed hydrological model based on grid-cell kinematic wave rainfall-runoff model (Kojima and Takara 2003, Apip et al. 2010). This model utilizes a set of stage-discharge relationship proposed by Takasao and Shiiba (1988) which was further developed for simulating unsaturated flow mechanism (Tachikawa et al. 2004) and its fundamental equations are similar to the OHDIS-KWMSS which has been applied to Japanese basins (Sayama and McDonnell 2009, Kim et al. 2009, Kim et al. 2010, and Kim et al. 2011). The original distributed model has been designed and successfully applied to steep humid and tropical basins (Sayama and McDonnell 2009, Kim et al. 2009, Sayama et al. 2003).

In this modelling framework, basin topography is represented based on digital elevation model (DEM) which is divided into an orthogonal matrix of square grid-cells. A square area on a node point of a DEM is considered as a sub-basin, which is called a grid-cell. The river basin is modeled as a network of grid-cell. Each grid-cell receives flows from upper grid-cells and rainfall on it. These grid-cells are connected to each other with a drainage path defined by the steepest of eight-direction. After deriving the flow direction information, a rectangular plane formed by two adjacent grid points is defined. Catchment topography is represented by a set of slope units. For each slope unit, its area, length and gradient are calculated. Discharge and water depth diffuse to the next grid-cell according to predefined eight-direction flow map and routine order determined in accordance with DEM and river channel network data. The hillslope flow is routed and given to the river flow routing model; then the river flow is routed to the outlet.

The continuity equation takes the flow rate of each grid-cell into account as follows:

$$\frac{\partial h}{\partial t} + \frac{\partial q}{\partial x} = r(t)\cos\phi \qquad [3]$$

where t is the time, ϕ is the slope angle, and r is the net rainfall intensity.

The model simulates three lateral flow mechanisms including: (1) subsurface flow through capillary pore (unsaturated flow), (2) subsurface flow through non-capillary pore (saturated flow) and (3) surface flow over the soil layer (overland flow). At each grid-cell, when the water depth is lower than the equivalent water depth d_m for the maximum volumetric water content in the unsaturated flow θ_m ($d_m = h^* \theta_m$), flow is simulated by Darcy law with degree of saturation, $(h_w/d_m)^{\beta}$, and an unsaturated hydraulic conductivity k_m. If the water depth exceeds the equivalent depth for unsaturated flow, the exceeded water flows as saturated subsurface flow that is simulated by Darcy law with saturated hydraulic conductivity k_a.

Once the water depth is greater than the soil layer h times effective porosity θ_a ($d_a = h^* \theta_a$), the water flows as surface flow, which is simulated by the Manning's equation. Herein, the basic assumption that the flow lines are parallel to the slope and the hydraulic gradient is equal to the slope. In addition, the kinematic wave model assumes that rainfall intensity always lower than infiltration rate capacity. Thus it does not consider the vertical water flow, the input rainfall data is directly added to subsurface flow or surface flow according to the water depth on the area where the rainfall dropped. Regarding this mechanism, overland flow happens if the depth of water exceeds the soil water capacity.

These three flow processes are represented by the following single set of stage-discharge relationships (Tachikawa et al. 2004) as follows:

$$q = \begin{cases} v_m d_m (\frac{h}{d_m})^{\beta}, & 0 \le h \le d_m \\ v_m d_m + v_a (h - d_m), & d_m < h \le d_a \\ v_m d_m + v_a (h - d_m) + \frac{\sqrt{i}}{n} (h - d_a)^m, & d_a < h \end{cases} \quad [4]$$

where v_m is the average velocity in the capillary layer (m s^{-1}), v_a is the average velocity in the non-capillary layer (m s^{-1}), i is the hillslope gradient and n is the roughness coefficient. Model parameters in the stage-discharge relationship are d_m, d_a, k_a, n, and β. The flow rate calculation is done combining the three flow processes (Equation 4) with the continuity equation (Tachikawa et al. 2004).

4.3 Ane Dam Routing Model

The Ane Dam main spillway is not controlled by any gates; therefore the discharge from the dam is a function of the water level inside the reservoir. In the model we set the grid cell where the dam is located to have the reservoir rules. All the water that goes into the grid cell where the dam is located is used to calculate the water balance in the reservoir using the Level Pool method. After calculating the volume inside we can use the relationship between elevation of the water surface and the volume in the reservoir to find the elevation of the water surface. Finally the discharge from the dam is calculated using the Spillway Stage-Discharge curve.

4.4 Model Calibration

For the CDRMV3 model we chose to calibrate 7 parameters: the manning roughness coefficient for the forest, the field area, the paddy field area and the river land use types; the hydraulic conductivity; total soil depth and the exponent constant of unsaturated flow. Based on previous studies (Sayama et al. 2003, Tachikawa et al. 2004, Apip et al. 2010, Apip et al. 2011) it was decided the feasible range for each parameter and randomly sampled parameter sets from this range (Table 4.1). The model was run 500 times for each event and the random sampling was done using a Monte Carlo generation with a uniform distribution. The objective function used to test the model was the Nash coefficient (Nash and Sutcliffe 1970) calculated as follows:

$$NSE(\theta) = 1 - \frac{\sum_{t=1}^{N} (Qobs_t - Qsim_t(\theta))^2}{\sum_{t=1}^{N} (Qobs_t - Q_{ave})^2} \quad [5]$$

where NSE(θ) is the Nash coefficient value for the parameter set θ, Qobst is the observed discharge at time t, Qave is the average of the observed discharge and Qsimt is the simulated discharge.

5. RESULTS AND DISCUSSION

The SVAT model was run to simulate snow accumulation and melt for the winters of 2010 and 2010-2011. The parameters of the CDRMV3 model were calibrated by using three different summer events. Finally the Snowmelt-runoff model was tested for three winter events.

5.1 Snow Accumulation and Melt

Figure 2 shows the snow accumulation and melt simulation results for the winters of 2010 and 2010-2011 for the point on the crest of the ARD. The SVAT model produces hourly values of snow depth, rainfall and total snowmelt. The patterns of daily snowmelt were well represented in the model during the ablation season. Peak snow accumulation usually happening in the end of January and beginning of February.

Table 1: Parameter spaces for the runoff model calibration.

Parameter	Description	Range		Dimension
		min.	max.	
n_{forest}	Manning roughness coefficient of the forest type land use	0.3	0.6	$m^{-1/3}s$
n_{field}	Manning roughness coefficient of the field type land use	0.1	0.2	$m^{-1/3}s$
n_{paddy}	Manning roughness coefficient of the paddy field type land use	0.2	0.4	$m^{-1/3}s$
n_{river}	Manning roughness coefficient of the river type land use	0.01	0.04	$m^{-1/3}s$
k_a	Hydraulic conductivity of saturated soil layer	0.004	0.0008	$mm\ s^{-1}$
d_a	Total non-capillary and capillary soil layer depth	200	800	mm
β	Exponent constant of unsaturated flow	3	10	–

In the 2010 winter period, the model overestimates snow depth and the time of snow disappearance is about 10 days late. In the winter of 2010-2011 peak snow depth is overestimated in about 80cm, however time of snow disappearance is well represented. The new snow density was assumed to be constant and of 100 kg m^{-3}. Since there was not any accounting for snowpack compaction, this could well be the reason for greater simulated snow depth than real.

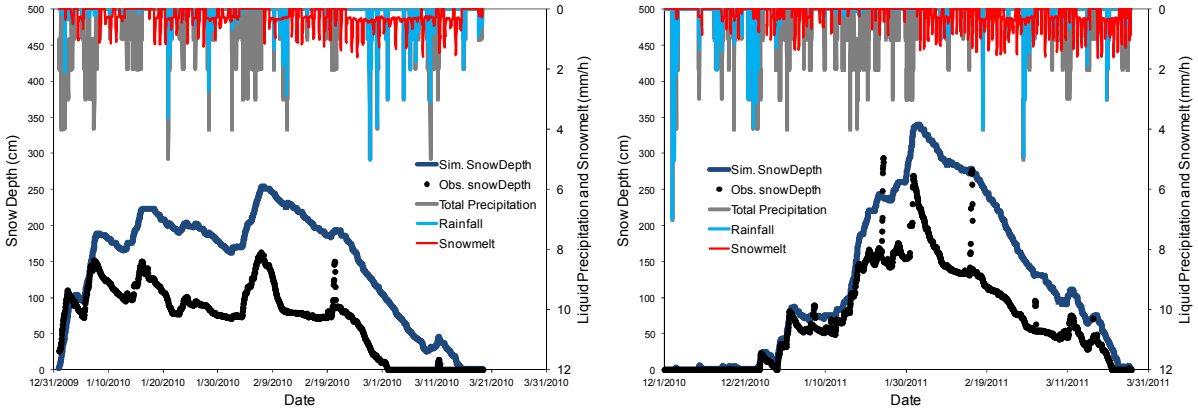

Figure 2: Simulated rainfall, snowmelt and snow depth for the 2 winters.

5.2 Runoff Model Calibration

The runoff model was calibrated by using dam inflow hydrographs for three summer events that happened in 14 June 2010 (Event 1), 18 June 2010 (Event 2) and 22 June 2010 (Event 3, Figure 3). The models were run 500 times for each event and the best parameter sets of each event were chosen to run the winter events. Event 1 obtained a best Nash value of 0.92, Event 2 of 0.96 and Event 3 of 0.94.

Using these model runs it is possible to identify the parameters to which the model is most sensitive. Considering all the events, the model was mostly sensitive to k_a, d_a and n_{river}. For the two smaller events (Event 1 and 2) the values of the total depth of capillary and non-capillary d_a were relatively high, this happens to compensate for a slower flows and smaller peaks. In Event 3, where peak discharge was much higher (30 m^3/s), d_a and n_{river} are relatively lower, this way there is faster runoff routing.

The patterns of wetting and drying of the soil can be represented by the model (bottom panel of Figure 4.3). It can be seen that even though Event 3 had a much higher peak, water in the soil was rapidly drained after the peak and did not saturated as much as Event 2. The differences are also related to the different rainfall patterns, where in Event 2 rainfall is more concentrated than Event 3. This type of uncertainty related to different parameter sets and wetter and drier events should be further investigated.

The simulated water level inside the dam, and consequently the outflow discharge, was overestimated for all the events. This indicates that the ARD reservoir might be too big for the use of the lumped Level Pool routing scheme. It is known that the Level Pool routing when compared to distributed ones usually overestimates the outflow discharge, however its computational simplicity is a great advantage. Besides that, it is possible that there are inaccuracies arising from the stage-volume and stage-discharge curves of the reservoir. Despite these problems, the recession curves fit very well with the observed one and the lumped routing scheme can be used with more confidence for long term discharge simulations applied in water resources management cases.

5.3 Snowmelt-Runoff Model

Snowmelt runoff was calculated for three selected winter events by using the SVAT model coupled with the cell distributed runoff model and the dam routing routine. For model testing, the calibrated parameters for the three summer events were used to run the three selected winter events: EventW1 (20 January 2010, Figure 4a); EventW2 (27 January 2010, Figure 4b); and Event W3 (17 February 2011, Figure 4c).

Event W1 and W2 had observed reservoir levels below 427.4 m, which is below the main spillway and the model cannot account for the discharge since there is no rule for the operation of the controlled outlet of the ARD. In these cases, the initial reservoir level was set to 427.4 m so the model could represent the outflow for the case in which the main spillway is working. Figure 4a-c shows that the model is very sensitive to snowmelt and rainfall. However, our confidence in the observed inflow data is very low due to river freezing, and that inflow observed data does not change with snowmelt inputs. Also in Event W3, reservoir inflow is much lesser than outflow which demonstrates problems with measurement equipment during winter time.

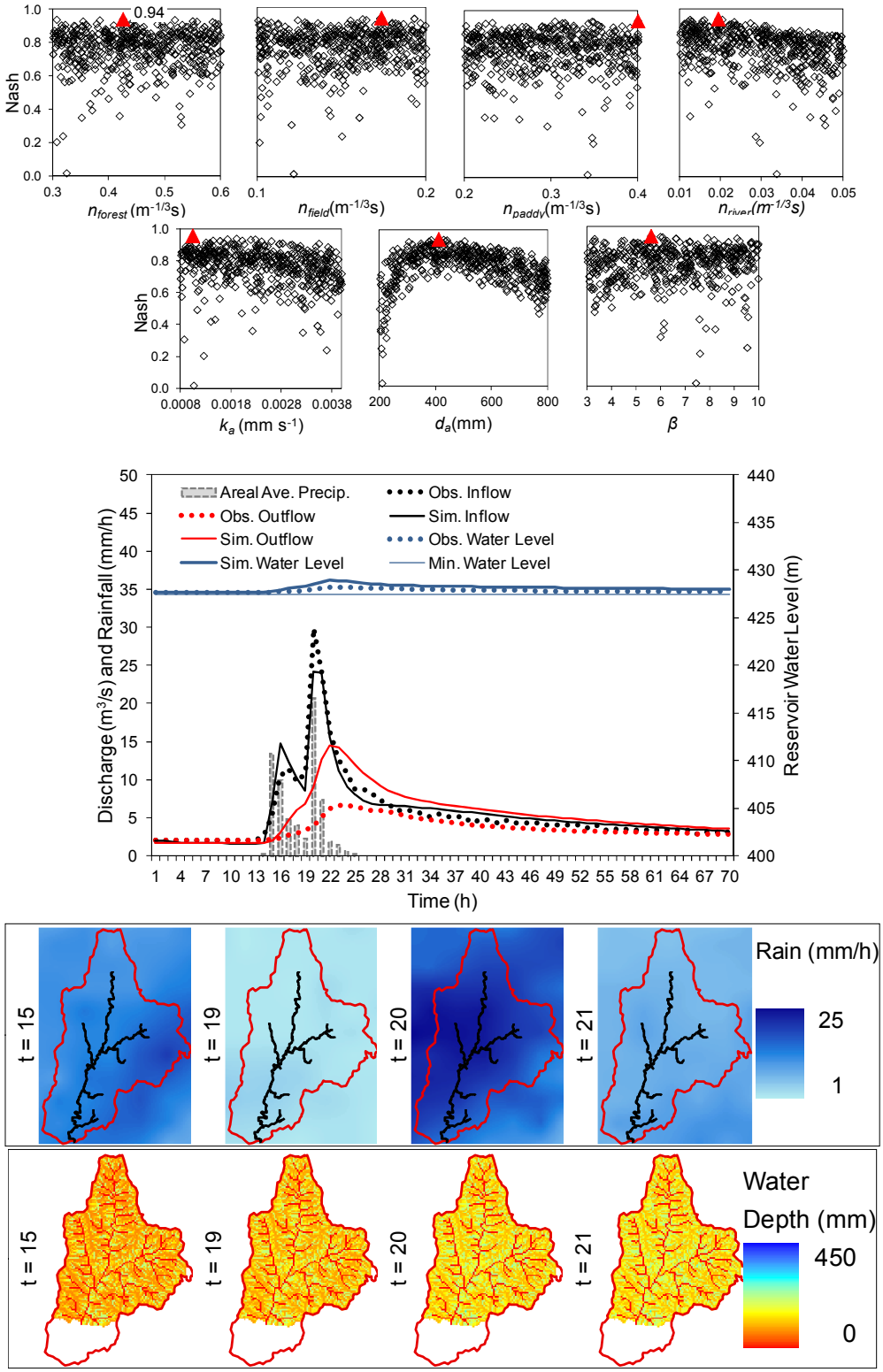

Figure 3: Plot of calibrated summer events (22Jun2010 10h - 25 Jun 2010 7h). Top panel showing parameter sensitivity. Bottom panels showing Radar AMeDAS rainfall and depth of water in the soil.

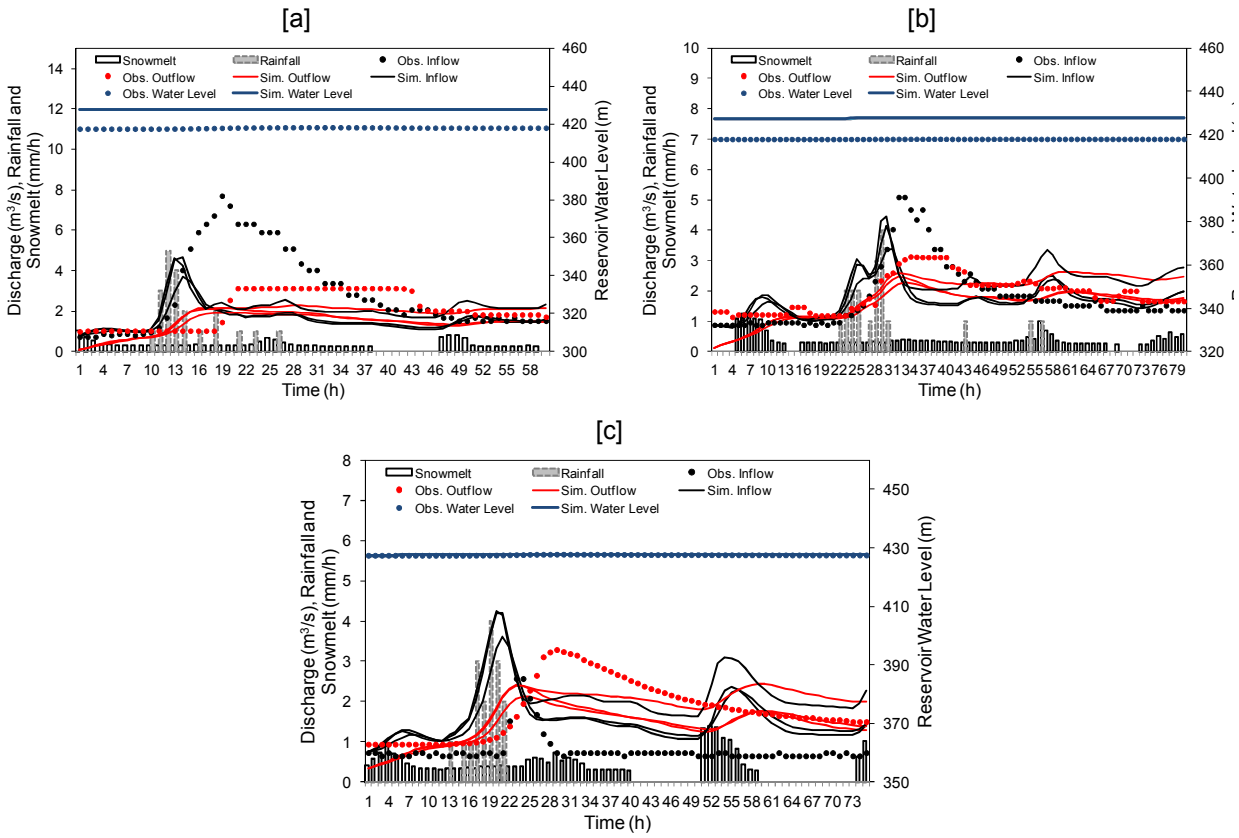

Figure 4: Plot of simulated winter event. [a] 20Jan2010 13h - 23Jan2010 1h. [b] 27Jan2010 5h - 30Jan2010 12h. [c] 17Feb2011 7h - 20Feb2011 9h.

6. CONCLUSIONS

This paper presents the modification and coupling of a SVAT model, a cell distributed runoff model and a Level Pool routing scheme in order to simulate snowmelt-runoff from the Ane River Dam catchment. Snow accumulation and melt were simulated by the SVAT model and its accumulation and depletion pattern represented well the observed snow depth at the crest of the Ane River Dam. The total snow depth was overestimated due to the constant snow density which was used in the model. The time of snow disappearance was well estimated for the winter of 2010-2011, however, it was 10 days late in the winter of 2010.

The runoff model considering the dam function was calibrated for three summer events and it was found that the three most sensitive model parameters are k_a, d_a and n_{river}. The simulated peak outflow from the dam was overestimated by the Level Pool scheme, but the recession curves were accurate. The use of the summer calibrated parameters for the three winter events demonstrates the developed snowmelt-runoff model sensitivity to snowmelt and rainfall. However, there are still verification limitations due to the quality of observed inflow data during the winter and the uncertain simulation of soil moisture patterns.

AKNOWLEDGEMENTS

The authors gratefully acknowledge Assoc. Prof Yoshinobu Sato for sharing SVAT model code and Assoc. Prof. Kenji Tanaka for sharing data. The first author received a PhD grant from The Ministry of Education, Culture, Sports, Science and Technology of Japan (MEXT). We also thank the financial support from The GCOE Program "Sustainability/Survivability Science for a Resilient Society Adaptable to Extreme Weather Conditions" (GCOE-ARS).

7. REFERENCES

Apip, Sayama, T., Tachikawa, Y. and Takara, K., 2011: Spatial lumping of a distributed rainfall-sediment-runoff model and its effective lumping scale. *Hydrological Processes* 26, 855–871.

Apip, Sayama, T., Tachikawa, Y., Takara, K. and Yamashiki, Y., 2010: Assessing sources of parametric uncertainty and uncertainty propagation in sediment runoff simulations of flooding, *Journal of Flood Risk Management* 3, 270–284.

Iida, Y., Okamoto, K., Ushio, T. and Oki, R., 2006: Simulation of sampling error of average rainfall rates in space and time by five satellites using radar-AMeDAS composites. *Geophysical Research Letters* 33, L01816.

Iwaki, M., Hida, Y., Ueno, K. and Saijyou, M., 2011: Observation of snow water equivalent in the North catchment area of Lake Biwa. *Lakes & Reservoirs: Research and Management* 16, 215–221.

Kim, S., Tachikawa, Y., Nakakita, E. and Takara, K., 2010: Hydrologic evaluation on the AGCM20 output using observed river discharge data. *Hydrological Research Letters* 4, 35–39.

Kim, S., Tachikawa, Y., Nakakita, E. and Takara, K., 2009: Reconsideration of reservoir operations under climate change: case study with Yagisawa Dam, Japan. *Annual Journal of Hydraulic Engineering* 53, 115–120.

Kim, S., Tachikawa, Y., Nakakita, E., Yorozu, K. and Shiiba, M., 2011: Climate change impact on river flow of the Tone River basin, Japan. *Annual Journal of Hydraulic Engineering* 55, 85–90.

Kitabake, N. and Obayashi, M., 1991: A study comparing Radar-AMeDAS precipitation chart with observed data of rain gauge network of Tokyo Metropolis. *Journal Meteorological Research* 43, 285-310.(in Japanese)

Kojima, T. and Takara, K., 2003: A grid-cell based distributed flood runoff model and its performance, Weather radar information and distributed hydrological modeling. *IAHS Publ.* 282, 234–240.

Kondo, J. and Xu, J., 1997: Seasonal variations in the heat and water balances for nonvegetated surfaces. *Journal of Applied Meteorology* 36, 1676–1695.

Kondo, J. and Yamazaki, T., 1990: A prediction model for snowmelt, snow surface temperature and freezing depth using a heat balance method. *Journal of Applied Meteorology* 29, 375–384.

Ma, X., Fukushima, Y., Hiyama, T., Hashimoto, T. and Ohata, T., 2000: A macro-scale hydrological analysis of the Lena River basin. *Hydrological Processes* 14, 639–651.

Ma, X., Fukushima, Y., Hashimoto, T., Hiyama, T. and Nakashima, T., 1999: Application of a simple SVAT model in a mountain catchment under temperate humid climate. *J. Japan Soc. Hydrol. & Water Resour.* 12, 285–294.

Ma, X., Hiyama, T., Fukushima, Y. and Hashimoto, T., 1998: A numerical model of heat transfer for permafrost regions. *J. Japan Soc. Hydrol. & Water Resour*. 11, 346–359.

Ma, X., Yasunari, T., Ohata, T., Natsagdorj, L., Davaa, G. and Oyunbaatar, D., 2003: Hydrological regime analysis of the Selenge River basin, Mongolia. *Hydrological Processes* 17, 2929–2945.

Makihara, Y., 1996. A method for improving radar estimates of precipitation by comparing data from radars and raingauges. *Journal of the Meteorological Society of Japan* 74, 459-480.

Nash, J.E. and Sutcliffe, J.V., 1970: River flow forecasting through conceptual models, Part I - A discussion of principles. *Journal of Hydrology* 10, 282–290.

Oki, R. and Sumi, A., 1994: Sampling simulation of TRMM rainfall estimation using radar-AMeDAS composites. *Journal of Applied Meteorology* 33, 1597-1608.

Oki, R., Sumi, A and Short, D.A., 1997: TRMM sampling of radar-AMeDAS rainfall using the threshold method. *Journal of Applied Meteorology* 36, 1480-1492.

Sato, Y., Ma, X., Xu, J., Matsuoka, M., Zheng, H., Liu, C. and Fukushima, Y., 2008: Analysis of long-term water balance in the source area of the Yellow River basin. *Hydrological Processes* 22, 1618–1629.

Sayama, T. and McDonnel, J.J., 2009: A new time-space accounting scheme to predict stream water residence time and hydrograph source components at the watershed scale. *Water Resources Research* 45, 1–14.

Sayama, T., Takara, K., and Tachikawa, Y., 2003: Reliability evaluation of rainfall-sediment-runoff models. *IAHS Publ*. 279, 131–141.

Shimizu, S., Oki, R. and Igarashi, T., 2001: Ground validation of radar reflectivity and rain rate retrieved by the TRMM precipitation radar. *Advanced Space Research* 28, 143-148.

Tachikawa, Y., Nagatani, G. and Takara, K., 2004: Development of stage-discharge relationship equation incorporating saturated-unsaturated flow mechanism. *Annual Journal of Hydraulic Engineering* (JSCE) 48, 7–12.

Takasao T, Shiiba M. 1988: Incorporation of the effect of concentration of flow into the kinematic wave equations and its application to runoff system lumping. *Journal of Hydrology* 102, 301–322.

Urita, S., Saito, H. and Matsuyama, H., 2011: Temporal and spatial discontinuity of radar/raingauge-analyzed precipitation that appeared in relation to the modification of its spatial resolution. *Hydrological Research Letters* 5, 37-41.

Xu, J., Haginoya, S., Saito, K. and Motoya, K., 2005: Surface heat balance and pan evaporation trends in Eastern Asia in the period 1971-2000. *Hydrological Processes* 19, 2161–2186.

Yamazaki, T. and Kondo, J., 1992: The snowmelt and heat balance in snow-covered forested areas. *Journal of Applied Meteorology* 31, 1322–1327.